Charge transfer in low-energy collisions of Be^{3+} and B^{4+} ions with He*

Kun Wang(王堃)[1], Yi-Zhi Qu(屈一至)[1,†], Chun-Hua Liu(刘春华)[2], Ling Liu(刘玲)[3], Yong Wu(吴勇)[3], H P Liebermann[4], and Robert J. Buenker[4]

[1] *School of Optoelectronics, University of Chinese Academy of Sciences, Beijing* 100049, *China*
[2] *School of Physics, Southeast University, Nanjing* 210094, *China*
[3] *Data Center for High Energy Density Physics, Institute of Applied Physics and Computational Mathematics, Beijing* 100088, *China*
[4] *Fachbereich C-Mathematik und Naturwissenschaften, Bergische Universitat Wuppertal, D-*42097 *Wuppertal, Germany*

(Received 25 April 2020; revised manuscript received 13 June 2020; accepted manuscript online 3 July 2020)

The nonradiative charge-transfer processes of $Be^{3+}(1s)/B^{4+}(1s)$ colliding with $He(1s^2)$ are investigated by the quantum-mechanical molecular orbital close-coupling (QMOCC) method from 10 eV/u to 1800 eV/u. Total and state-selective cross sections are obtained and compared with other results available. Although the incident ions have the same number of electrons and collide with the same target, their cross sections are different due to the differences in molecular structure. For $Be^{3+}(1s) + He(1s^2)$, only single-electron-capture (SEC) states are important and the total cross sections have a broad maximum around $E = 150$ eV/u. While for $B^{4+}(1s) + He(1s^2)$, both the SEC and double-electron-capture (DEC) processes are important, and the total SEC and DEC cross sections decrease rapidly with the energy decreasing.

Keywords: electron capture processes, low energy collision, QMOCC, $Be^{3+}(1s)/B^{4+}(1s) + He$

PACS: 34.70.+e, 34.20.−b **DOI:** 10.1088/1674-1056/aba276

1. Introduction

In the last few decades, the study of achieving controlled and sustained nuclear fusion has attracted much attention,[1,2] one of the most effective ways is to use the tokamaks. In the edge plasmas of many tokamaks, beryllium and boron are considered as important impurity ions. e.g., layers containing boron are formed in the plasma from boron-doped graphites due to boronization of the vessel walls,[3] while in the International Thermonuclear Experimental Reactor (ITER), beryllium is used as a armor material for the first wall.[4] Especially, the charge-exchange processes of Be^{q+} ions with helium atoms are considered to be the main 'poison' processes to reduce temperature. Therefore, the information of the cross sections and the comprehensive knowledge of the charge-exchange processes between Be^{q+}, B^{q+} ions with He are essential for simulation and diagnosis of tokamak plasmas.

Since the temperature of typical tokamak edge plasma is below 500 eV, the data of cross sections for charge transfer processes in low-energy collisions of these systems are required. Up until now, in the low energy region, the charge-transfer processes of Be^{3+}/B^{4+} colliding with He atoms have been studied theoretically by the earlier works.[5–10] The only experimental study below 1 keV/u is for B^{4+}+ He by Iwai *et al.*[11] We should mention that controversy remains among these works.

In this work, the charge-transfer processes of the Be^{3+}/B^{4+}+ He collision systems have been studied in the energy range 10–1800 eV/u by using the quantum-mechanical molecular orbital close-coupling (QMOCC) method. The adiabatic potentials, radial and rotational coupling-matrix elements, which are necessary in the dynamics calculation, have been computed by using the *ab initio* multireference single- and double-excitation configuration-interaction (MRD-CI) method.[12,13]

The present article is organized as follows. In the next section, the molecular potential and coupling data are presented. In Section 3, we briefly outline the theoretical methods. The results and discussion of the scattering calculations are presented in Section 4, followed by a brief summary in Section 5. Atomic units are used in the remaining part of this article, unless explicitly indicated otherwise.

2. Molecular structure calculations

2.1. $BeHe^{3+}$ molecular ion

In the present work, the basis sets used for both the beryllium and helium atoms are the correlation-consistent polarized valence quadruple-zeta (cc-pVQZ) Gaussion basis sets,[14,15] a diffuse (1s1p) set has been added for beryllium. Ultimately, the basis set (13s, 7p, 3d, 2f) contracted to [6s, 5p, 3d][14] is used for beryllium, while (7s, 3p, 2d, 1f) contracted to the [4s, 3p, 2d] basis set[15] is for helium. A selection threshold of 1.0×10^{-8} Hartree[12,16] is used for $BeHe^{3+}$ molecular ions,

*Project supported by the National Natural Science Foundation of China (Grant Nos. 11774344, 11474033, and 11574326) and the National Key Research and Development Program of China (Grant No. 2017YFA0402300).

†Corresponding author. E-mail: yzqu@ucas.ac.cn

and the spin–orbit interactions are not considered because the influence is small. As shown in Table 1, the states below the ionization threshold $Be^{2+}(1s^2) + He^{2+}$ should not be important because of the large energy gaps (over 74.891 eV) with the initial state $Be^{3+}(1s\ ^2S) + He(1s^2)$. By using the MRD-CI package,[12,13] *ab initio* multireference configuration interaction calculations have been performed for adiabatic potential curves, including six $^2\Sigma$ states and two $^2\Pi$ of the $BeHe^{3+}$ system at internuclear distances from 1.0 a.u. to 100.0 a.u. Compared to the experimental atomic energies[17] in the asymptotic region, the discrepancy of our calculated results is within 0.036 eV, which would be sufficient for getting the right potential curves, the radial coupling and the rotational coupling matrices. So that for the scattering calculations, this accuracy level is adequate for treating the present dynamics of $Be^{3+}(1s) + He(1s^2)$ collisions.[18]

Table 1. Asymptotic separated-atom energies for the states of $BeHe^{3+}$. The bold $5\ ^2\Sigma$ represents the initial state.

Molecular states	Asymptotic atomic states	Energy/eV		
		MRD-CI	Ref. [17]	Error
$X\ ^2\Sigma$	$Be^{2+}(1s^2\ ^1S) + He^+(1s)$	−129.149	−129.309	0.160
$A\ ^2\Sigma$	$Be^+(1s^2 2s\ ^2S) + He^{2+}$	−93.090	−93.102	0.012
.....				
	$Be^+(1s^2\varepsilon l) + He^{2+}$		−74.891	
$1\ ^2\Sigma$	$Be^{2+}(1s2s\ ^3S) + He^+(1s)$	−10.707	−10.717	0.010
$2\ ^2\Sigma$	$Be^{2+}(1s2s\ ^1S) + He^+(1s)$	−7.655	−7.658	0.003
$3\ ^2\Sigma, 1\ ^2\Pi$	$Be^{2+}(1s2p\ ^3P^0) + He^+(1s)$	−7.388	−7.388	0.000
$4\ ^2\Sigma, 2\ ^2\Pi$	$Be^{2+}(1s2p\ ^1P^0) + He^+(1s)$	−5.603	−5.640	0.037
$5\ ^2\Sigma$	**$Be^{3+}(1s\ ^2S) + He(1s^2)$**	**0**	**0**	**0**
$6\ ^2\Sigma$	$Be^{2+}(1s3s\ ^3S) + He^+(1s)$	9.731	9.700	0.031

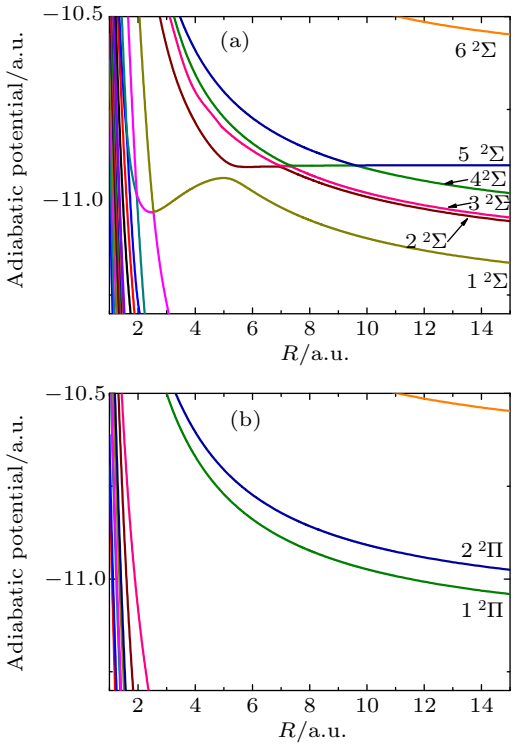

Fig. 1. Potential curves of $BeHe^{3+}$ molecular ions refer to Table 1.

The radial coupling matrix elements between molecular states of the same symmetry have been calculated by the finite difference technique

$$A_{ij}^R = \langle\psi_i|\frac{\partial}{\partial R}|\psi_i\rangle = \lim_{\Delta R\to 0}\frac{1}{\Delta R}\langle\psi_i(R)|\psi_i(R+\Delta R)\rangle, \qquad (1)$$

with a step size of 0.0002 a.u. While the rotational couplings $A_{ij}^\theta = \langle\psi_i|iL_y|\psi_j\rangle$ between states of angular momentum $\Delta\Lambda = \pm 1$ have been calculated directly from the angular momentum tensor.

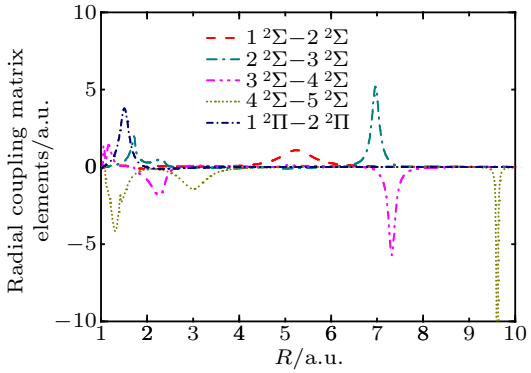

Fig. 2. Radial coupling matrix elements for $BeHe^{3+}$.

The adiabatic potential curves of $BeHe^{3+}$ molecular ions are presented at internuclear distance $R = 1.0$–15.0 a.u. in Fig. 1. The $5\ ^2\Sigma$ state represents the initial channel for the $Be^{3+}(1s) + He(1s^2)$ collision system. The radial coupling matrix elements for $BeHe^{3+}$ are displayed in Fig. 2. Obviously, the positions of the peaks are consistent with the avoided crossings observed in Fig. 1. In particular, there is a strong coupling between $2\ ^2\Sigma$ and $1\ ^2\Sigma$ state at internuclear distances ~ 5.4 a.u., which may drive directly the transition to the $Be^{2+}(1s2s\ ^3S) + He^+(1s)$ exit state. Note that the coupling between the $2\ ^2\Sigma$ and $3\ ^2\Sigma$ states has a peak at $R \sim 2.4$ a.u. which is much weaker, and it will be important only at high collision energies. Moreover, clear and narrow avoided crossings be-

tween 2 $^2\Sigma$–3 $^2\Sigma$, 3 $^2\Sigma$–4 $^2\Sigma$, and 4 $^2\Sigma$–5 $^2\Sigma$ are observed at $R \sim 6.9$ a.u., 7.3 a.u., and 9.6 a.u. (see Fig. 1), respectively. The corresponding radial coupling matrix elements are very sharp, as shown in Fig. 2.

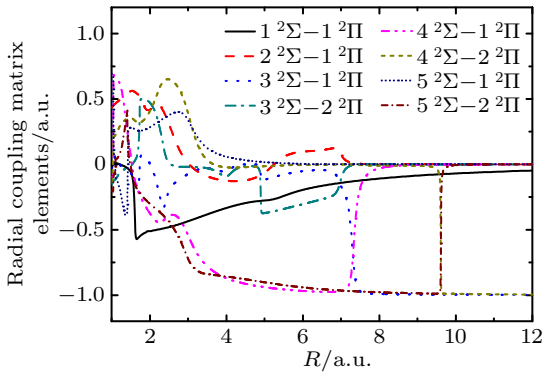

Fig. 3. Rotational coupling matrix elements for $BeHe^{3+}$.

Also, the most important rotational couplings are presented in Fig. 3. It can be seen that the rotational couplings are not smooth, since the adiabatic interactions are strong near the positions of the avoided crossings. In the region of $R > 10.0$ a.u., the asymptotical value of the 3 $^2\Sigma$–1 $^2\Pi$ couplings is about -1.0 a.u., and it may affect the population to the $Be^{2+}(1s2p\ ^3P^0) + He^+(1s)$ exit state, while the strong couplings between 4 $^2\Sigma$–2 $^2\Pi$ play an important role for the population to the $Be^{2+}(1s2p\ ^1P^0) + He^+(1s)$.

2.2. BHe^{4+} molecular ion

The $B^{4+}(1s\ ^2S) + He(1s^2)$ scattering system has the same electron numbers with $Be^{3+}(1s\ ^2S) + He(1s^2)$. For comparison, the adiabatic potentials and coupling matrix elements have also been obtained by using the MRD-CI method. For the B atom, we have used the correlation-consistent polarized valence quadruple-zeta (cc-pVQZ) Gaussion basis sets[14,15] with a diffuse (5s4p3d2f) set, the (17s, 10p, 6d, 4f) contracted to [10s, 8p, 6d, 4f] basis set[14] is employed for boron. While for the He atom, the same basis set which was used in the calculation of the $BeHe^{3+}$ ion[15] is employed for helium. Like the $Be^{3+}(1s\ ^2S) + He(1s^2)$ system, the states below the ionization threshold $B^{3+}\ (1s^2) + He^{2+}$ should not be important either because of the large energy gaps (over 180.366 eV) with the initial state $B^{4+}(1s\ ^2S) + He(1s^2)$ as shown in Table 2. The structure of the BHe^{4+}system has been computed by using the MRD-CI method, thirteen $^2\Sigma$, one $^2\Delta$, and seven $^2\Pi$ states have been performed. The asymptotic energies in the separated-atom limit of the considered states are shown in Table 2 and compared with the experimental data.[17] The 13 $^2\Sigma$ state represents the initial channel of the $B^{4+}(1s\ ^2S) + He(1s^2)$ collision system. The largest error in the relative asymptotic energies of this system is about 0.179 eV.

The calculated adiabatic potentials for internuclear distances $R = 1.0$–15.0 a.u. are plotted in Fig. 4. Notably, four sharp avoided crossings between the 13 $^2\Sigma$ state and the 6–9 $^2\Sigma$ states at $R \sim 5.6$ a.u., 6.5 a.u., 7.8 a.u., and 12.0 a.u. have been replaced by real crossings, respectively. Figures 5(a)–5(f) display some important radial and rotational couplings, respectively. Differing from the $Be^{3+}(1s\ ^2S) + He(1s^2)$ system, there are no effective avoided crossings between the initial state with others in the region of $R > 4.0$ a.u., so that no strong nonadiabatic coupling would be induced at low collision energy.

Table 2. Asymptotic separated-atom energies for the states of BHe^{4+}. The bold 13 $^2\Sigma$ represents the initial state.

Molecular states	Asymptotic atomic states	Energy/eV		
		MRD-CI	Ref. [17]	Error
X $^2\Sigma$	$B^{3+}(1s^2\ ^1S) + He^+(1s)$	−234.700	−234.784	0.084
A $^2\Sigma$	$B^{2+}(1s^22s\ ^2S) + He^{2+}$	−218.190	−218.297	0.107
.....				
	$B^{2+}(1s^2\varepsilon l) + He^{2+}$		−180.366	
1 $^2\Sigma$	$B^{3+}(1s2s\ ^3S) + He^+(1s)$	−36.277	−36.219	−0.058
2 $^2\Sigma$	$B^{3+}(1s2s\ ^1S) + He^+(1s)$	−32.041	−31.982	−0.059
3 $^2\Sigma$, 1 $^2\Pi$	$B^{3+}(1s2p\ ^3P^0) + He^+(1s)$	−31.882	−31.833	−0.049
4 $^2\Sigma$, 2 $^2\Pi$	$B^{3+}(1s2p\ ^1P^0) + He^+(1s)$	−29.209	−29.222	0.013
5 $^2\Sigma$	$B^{2+}(1s2s^2\ ^2S) + He^{2+}$	−25.548	−25.567	0.019
6 $^2\Sigma$, 3 $^2\Pi$	$B^{2+}(1s(^2S)2s2p(^3P^0)\ ^2P^0) + He^{2+}$	−19.142	−19.167	0.025
7 $^2\Sigma$, 4 $^2\Pi$	$B^{2+}(1s(^2S)2s2p(^1P^0)\ ^2P^0) + He^{2+}$	−16.243	−16.321	0.078
8 $^2\Sigma$, 5 $^2\Pi$, 1 $^2\Delta$	$B^{2+}(1s2p^2\ ^2D) + He^{2+}$	−13.944	−14.070	0.126
6 $^2\Pi$	$B^{2+}(1s2p^2\ ^2P) + He^{2+}$	−13.035	−13.100	0.065
9 $^2\Sigma$	$B^{2+}(1s2p^2\ ^2S) + He^{2+}$	−9.078	−9.257	0.179
10 $^2\Sigma$	$B^{3+}(1s3s\ ^3S) + He^+(1s)$	−1.424	−1.354	−0.070
11 $^2\Sigma$	$B^{3+}(1s3s\ ^1S) + He^+(1s)$	−0.297	−0.234	−0.063
12 $^2\Sigma$, 7 $^2\Pi$	$B^{3+}(1s3p\ ^3P^0) + He^+(1s)$	−0.236	−0.178	−0.058
13 $^2\Sigma$	**$B^{4+}(1s\ ^2S) + He(1s^2)$**	**0**	**0**	**0**

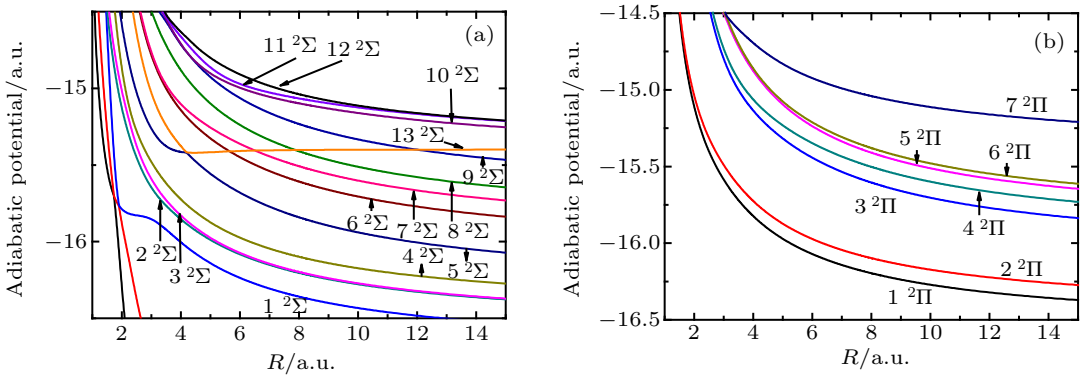

Fig. 4. Potential curves of BHe^{4+} molecular ions refer to Table 2.

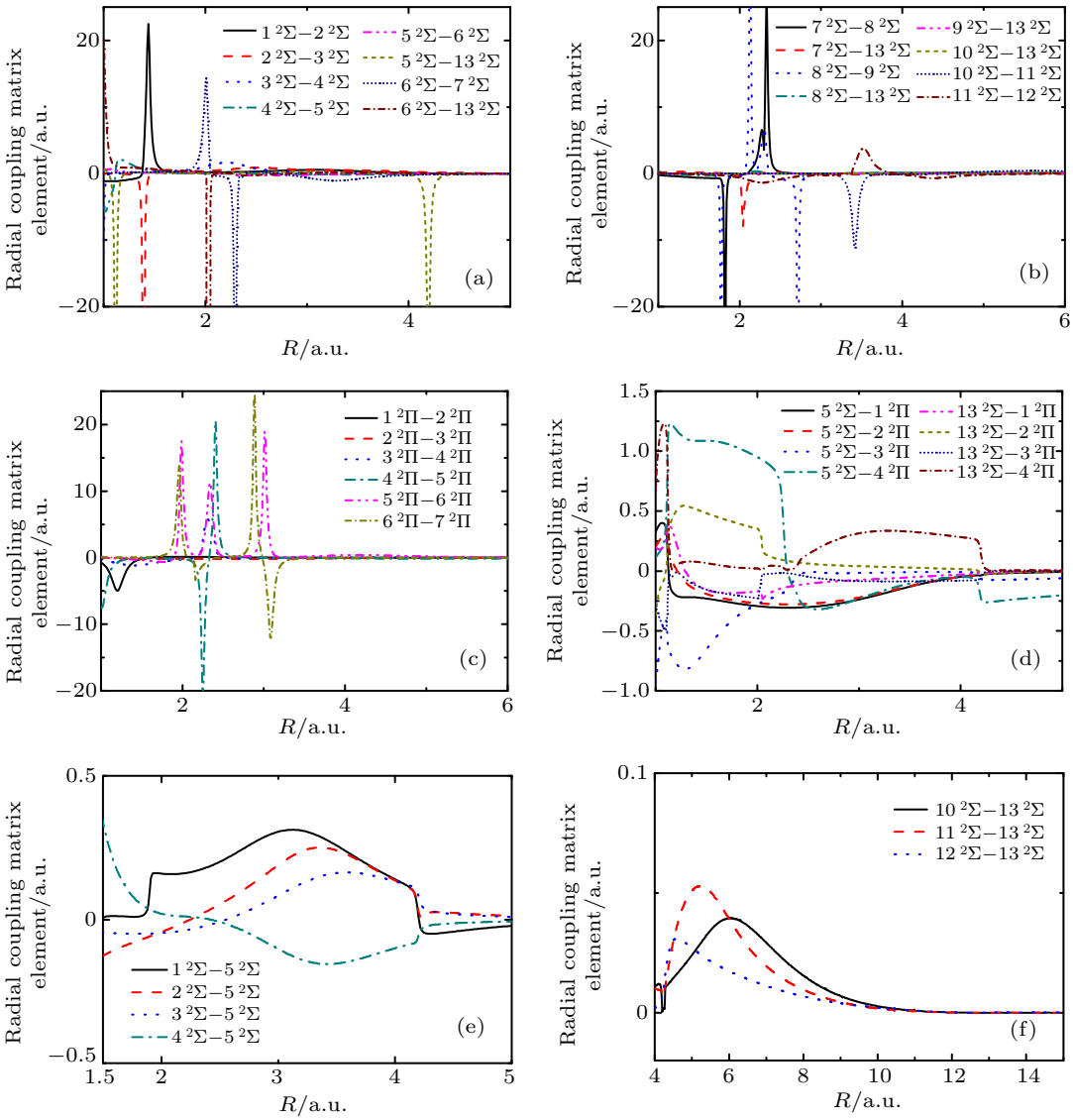

Fig. 5. Coupling matrix elements for BHe^{4+}: (a) and (b) radial coupling matrix element between $^1\Sigma^+$ states, (c) radial coupling matrix element between $^1\Pi$ states, (d) rotational coupling matrix element between $^1\Sigma^+$ and $^1\Pi$ states, (e) and (f) some important detailed radial coupling matrix element between exit states with the initial state.

More interestingly, some relatively weak couplings would make contributions to the population of B^{3+}(1s2l, 3l) + He^+(1s) exit states as shown in Figs. 5(e) and 5(f). It can be seen from Fig. 4 that when the internuclear distance R is less than 4.0 a.u., with decreasing R, the potentials for 1–4 $^2\Sigma$ and 5 $^2\Sigma$ become more and more close, which implies that the radial couplings shown in Fig. 5(e) between them may be important in high collision energy region. Broad and relatively weak peaks can be seen from Fig. 5(f), and may contribute to the populations of B^{3+}(1s3l) from the low energy region.

2.3. Comparison between $BeHe^{3+}$ and BHe^{4+} systems

In the molecular structure calculations of $BeHe^{3+}$ and BHe^{4+} molecular ions, although both have the same number of electrons, the initial and the most important exit states have large energy gaps (larger than 64 eV) with the ionization threshold as shown in Tables 1 and 2, they still have some differences which may lead to different results in the collision dynamics.

As shown in Table 1, for the $BeHe^{3+}$ system, the main electron capture process should be the SEC process. While the DEC process should be weak here, since all the double-electron capture states have large energy gaps with the initial state. While for the BHe^{4+} molecular ion, it can be seen from Table 2 that not only the SEC process but also the DEC process may be important in the considered energy region, since the asymptotic separated-atom energies of the states, SEC and DEC to, are not far from the initial state $B^{4+}(1s\ ^2S) + He(1s^2)$. And this system is more complex because the DEC channels lie energetically among the SEC channels.

Moreover, for the $BeHe^{3+}$ system, the main SEC processes are to the $Be^{2+}(1s2l) + He^{+}(1s)$ states, the $Be^{2+}(1s3l) + He^{+}(1s)$ states are insignificant as their energies lie relatively high above the initial state $Be^{3+}(1s\ ^2S) + He(1s^2)$. But for the BHe^{4+} molecular ion, Table 2 indicates that the energy levels of $B^{3+}(1s3l) + He^{+}(1s)$ states are very close to the initial state $B^{4+}(1s\ ^2S) + He(1s^2)$ at large internuclear distances, and may make contributions in the collision dynamics.

Furthermore, we compare the radial coupling matrix elements which are shown in Figs. 2 and 5. For the $BeHe^{3+}$ system, it can be observed that the couplings between the initial $2\ ^2\Sigma$ state with the $1\ ^2\Sigma$ state have a broad peak at internuclear distances $R \sim 5.4$ a.u. and it would drive directly the transition to the $Be^{2+}(1s2s\ ^3S) + He^{+}(1s)$ exit state. Also, the coupling between the $2\ ^2\Sigma$ and $3\ ^2\Sigma$ states has a peak at about 2.4 a.u., which will make contributions in the collision dynamics at high collision energies. However, the radial couplings of BHe^{4+}, as shown in Fig. 5, indicate that there is no effective coupling between the initial state with other molecular states.

3. Scattering calculations

In the present work, the quantum-mechanical molecular orbital close-coupling (QMOCC) approach is used to describe the charge transfer processes. This method has been formulated and described by Zygelman and Dalgarno[19] and Kimura and Lane,[20] here we only give a brief summary. In the adiabatic representation, transitions between channels are driven by radial and rotational (A^R and A^θ) couplings of the vector potential $\boldsymbol{A}(\boldsymbol{R})$, where $\boldsymbol{R}$ is the internuclear distance vector. Because the first and the second derivatives are included in the adiabatic description, using the unitary transformation[19,21] would be numerically convenient from the adiabatic representation to a diabatic representation

$$\boldsymbol{U}(R) = \boldsymbol{W}(R)[\boldsymbol{V}(R) - \boldsymbol{P}(R)]\boldsymbol{W}^{-1}(R), \tag{2}$$

where $\boldsymbol{U}(R)$ is the adiabatic potential matrix, $\boldsymbol{V}(R)$ is the diagonal adiabatic potential, $\boldsymbol{W}(R)$ is a unitary transformation matrix, and $P(R)$ is the rotational matrix of the vector potential $A(\boldsymbol{R})$.

By using the log-derivative method of Johnson,[22] the $\boldsymbol{K}$ matrix which is obtained from the scattering amplitude after a partial-wave decomposition[19] could be extracted. Thus the scattering matrix $\boldsymbol{S}$ is obtained,

$$\boldsymbol{S}_J = [\boldsymbol{I} + \mathrm{i}\boldsymbol{K}_J]^{-1}[I - \mathrm{i}\boldsymbol{K}_J]. \tag{3}$$

The charge-capture cross section from the initial channel i to the final channel j is given by

$$\sigma_{(i\to j)} = \frac{\pi}{k_i^2} \sum_J^{(2J+1)|S_J|^2_{i,j}}, \tag{4}$$

where k_i denotes the initial momentum.

The electron translation factors (ETFs),[23] which are expected not to be ignored for collision energies above 1 keV/u,[24] are taken into account. Allowance for the consideration of translation effects in the collision dynamics is made by introducing appropriate reaction coordinates,[25,26] we transform the radial and rotational coupling matrix elements between the states ψ_K and ψ_L into[27]

$$\begin{aligned} &\langle\psi_K|\partial/\partial R - (\varepsilon_K - \varepsilon_L)z^2/2R|\psi_L\rangle, \\ &\langle\psi_K|\mathrm{i}L_y + (\varepsilon_K - \varepsilon_L)zx|\psi_L\rangle, \end{aligned} \tag{5}$$

respectively, where ε_K and ε_L are the electronic energies of states ψ_K and ψ_L, and z^2 and zx are the components of the quadrupole moment tensor. This modification is similar to the one resulting from the application of the common ETF method in form.[23]

4. Results and discussion

4.1. $Be^{3+}(1s) + He(1s^2) \to Be^{2+} + He^{+}$

As shown in Fig. 6, the total non-radiative charge-transfer cross sections (including the ETF effects) are calculated in the energy range of 10–1800 eV/u, and they are in general agreement with those of Suzuki *et al.*[5] by using the semiclassical molecular-state expansion method in the overlapping energy range. It is found that there is a broad maximum peak at around $E = 150$ eV/u, while Suzuki's results decrease with the collision energy increasing in their whole energy region. For $E < 200$ eV/u, the QMOCC results are somewhat lower, especially for $E < 100$ eV/u. Due to the straight-line trajectory applied for nuclear motion, the computational limit of the semi-classical method is at this energy region, while in the QMOCC method, all electrons and nucleus are treated quantum mechanically. In general, the QMOCC results are more

reliable than the semi-classical ones for the energy less than about 1 keV/u, especially for collision energy less than several hundred eV/u.[28,29]

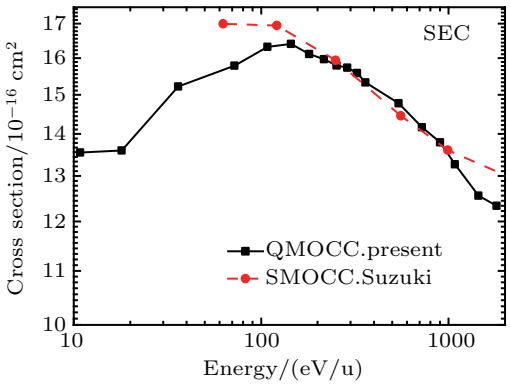

Fig. 6. Comparison between the present SEC cross sections for the $Be^{3+}(1s) + He(1s^2)$ collision with other theoretical results. Present QMOCC calculation considering the ETF effects (solid line with filled squares); semi-classical molecular orbital close coupling (SMOCC) results of Suzuki *et al.*[5] (dashed line with filled circles).

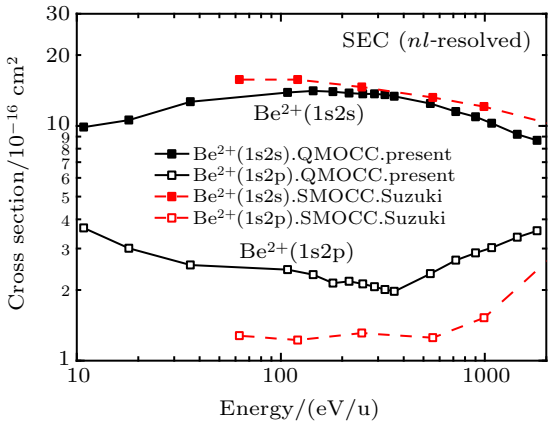

Fig. 7. State-selective cross sections of present QMOCC results (considering the ETF effects) and the results of Suzuki *et al.*[5] for electron capture to the 1s2s and 1s2p states of Be^{2+} ions.

For further study, the state-selective cross sections for electron capture to Be^{2+}(1s2s) and Be^{2+}(1s2p) states are shown in Fig. 7 and compared with those of Suzuki *et al.*[5] Our QMOCC results agree with the semiclassical ones[5] for those dominant capture processes to Be^{2+}(1s2s) due to the strong radial coupling between 1 $^2\Sigma$ and 2 $^2\Sigma$ states at around 5.4 a.u., as mentioned in Section 2. The cross section has a broad maximum at relatively low collision energies ($\sim$ 150 eV/u) because of the appearing of this coupling at relatively large distances. On the other hand, the cross section of the Be^{2+}(1s2p) state is relatively small except in the lower-energy or higher-energy region. For energy less than $\sim$ 100 eV/u, the rotational 3 $^2\Sigma$–1 $^2\Pi$ and 4 $^2\Sigma$–2 $^2\Pi$ couplings make contributions to the population of Be^{2+}(1s2p) states. For $E > 200$ eV/u, with the energy increasing, the cross sections to Be^{2+}(1s2p) states increase, because in the small R region, the potentials for 3–5 $^2\Sigma$ and 1, 2 $^2\Pi$ states become very close with decreasing R, the radial and rotational couplings between them make contributions in the high collision energy region.

In Fig. 8, cross sections for electron capture to singlet and triplet states of Be^{2+} ions are compared with those of Suzuki *et al.*[5] It can be observed that the cross sections of the electron capture for the triplet formation are dominant, it is consistent with the previous results that the electron capture to the Be^{2+}(1s2s ^{3}S) state is dominant. The trend of the cross section for the triplet states agrees well with Suzuki's result in the overlapping energy range. Compared with the triplet states, the cross sections for the singlet states are not important, e.g., at 100 eV/u, 300 eV/u, and 1000 eV/u, the cross section is about one fifth, one fourth, and one third of that for the triplet states, respectively. For the singlet formation, in 200–1000 eV/u, the trend of the cross sections is different. Around 500 eV/u, there is a relatively smaller peak due to the contributions from the radial 2 $^2\Sigma$–3 $^2\Sigma$ couplings, which has a relatively weaker peak at $R \sim 2.4$ a.u. As mentioned previously, the QMOCC results should be more reliable than the semi-classical ones in this energy region.[28,29]

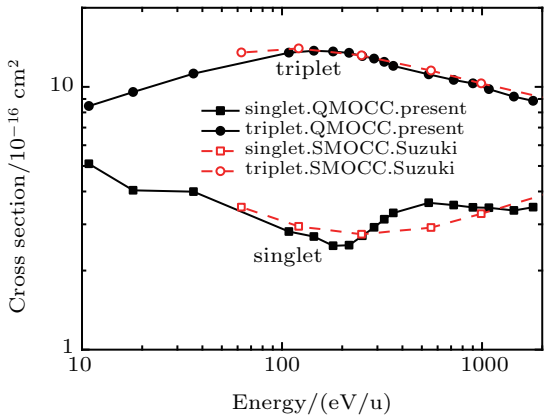

Fig. 8. Cross sections of present QMOCC results (considering the ETF effects) and the results of Suzuki *et al.*[5] for electron capture to singlet and triplet states of Be^{2+} ions.

4.2. $B^{4+}(1s) + He(1s^2) \rightarrow B^{3+} + He^+$

For comparison, we have also calculated cross sections for the $B^{4+}(1s) + He(1s^2)$ collision system using the QMOCC method (including the ETF effects) in the energy range 18–1700 eV/u. The total SEC cross sections are shown in Fig. 9 and compared with the experimental results of Iwai *et al.*,[11] the atomic-orbital close-coupling (AOCC) results of Hansen *et al.*,[7] the semi-classical results of Fritsch *et al.*[8] and Shimakura *et al.*[10] In the overlapping energy range, our results are in good agreement with the semi-classical results of Fritsch *et al.*[8] and the experimental data within their error bars,[11] except at $E \sim 1$ keV/u, the result is 20% lower than the experimental measured value. For $E < 500$ eV/u, the AOCC results of Hansen *et al.*[7] are larger than ours and other theoretical results.[10] And our results are in good agreement with the results of Shimakura *et al.*[10] for the collision energy from 200 eV/u to 500 eV/u, but are larger in the lower energy region, and smaller in the higher energy region. There are two

reasons for the differences, (i) full electron molecular method is used in our calculations, while the other calculations[7,8,10] used model potentials with only two-electron atomic orbitals considered. (ii) In general, the QMOCC results are more reliable for the energy less than ~ 1 keV/u, while the straight-line trajectory approximation of the semi-classical method starts to fail below several hundred eV/u.[28,29] In our considered energy region, as the energy increases, the cross section also increases because in this system, no strong coupling exists at large internuclear distances, which has been discussed in Subsection 2.2. Note that the values of the cross sections remain the same from about 60 eV/u to 150 eV/u, which can be explained by the state-selective SEC cross sections.

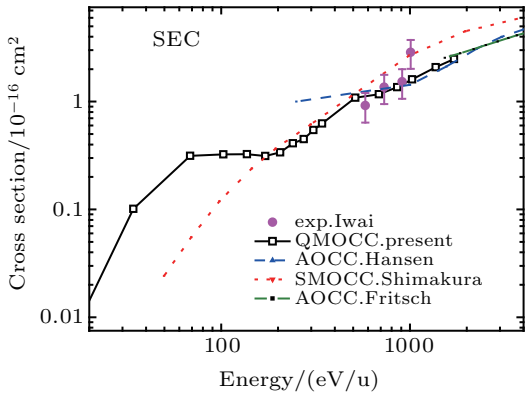

Fig. 9. Comparison between the present SEC cross sections for the $B^{4+}(1s)$ + $He(1s^2)$ collision with other theoretical[7,8,10] and experimental[11] results. Present QMOCC calculation considering the ETF effects (solid line with open squares); AOCC results of Hansen *et al.*[7] (dashed line); semi-classical results of Fritsch *et al.*[8] (dash dotted line) and Shimakura *et al.*[10] (dotted line). Experimental results of Iwai *et al.*[11] (filled circles with error bars).

As shown in Fig. 10, the state-selective SEC cross sections are compared with other available theoretical results. In the considered energy region, as the energy increases, the cross sections to 2s and 2p states are also increasing because (i) just as mentioned in Section 2, no effective avoided crossings have been found between the initial state with 2s and 2p states in the large R region ($R > 4.0$ a.u.), (ii) when the internuclear distance $R < 4.0$ a.u., the potentials for 1–4 $^2\Sigma$ and the initial state become very close with decrease of R, and the radial couplings (Fig. 5(e)) between them make contributions in the high collision energy region. And the cross sections for capture to the 2s state of the B^{3+} ion are lower than those to the 2p state, but the cross sections for capture to the 3l states are relatively small in the whole energy region, this trend is consistent with other theoretical results.[7,8,10] For $E > 70$ eV/u, the cross sections to the 3l states become nearly constant, since the broad and relatively weak couplings (Fig. 5(f)) make contributions here. However, there are some differences among ours and other theoretical results. For $E < 500$ eV/u, the AOCC results for capture to 2p state by Hansen *et al.*[7] are obviously larger than other theoretical results, e.g., it is nearly 6 times our result at $E = 250$ eV/u. And our QMOCC results for capture to 2s and 3l states are larger than the other results,[7,10] e.g., for capture to 2s states, at $E = 500$ eV/u, our result is about three times the results by Shimakura *et al.*,[10] with the energy decreasing, the difference goes to about 80 times at $E = 150$ eV/u. This is most probably because of the different methods. Generally, the QMOCC results are more reliable for the energy less than about 1 keV/u. Note that our results are not smooth, it is because of the complex radial and rotational couplings between states.

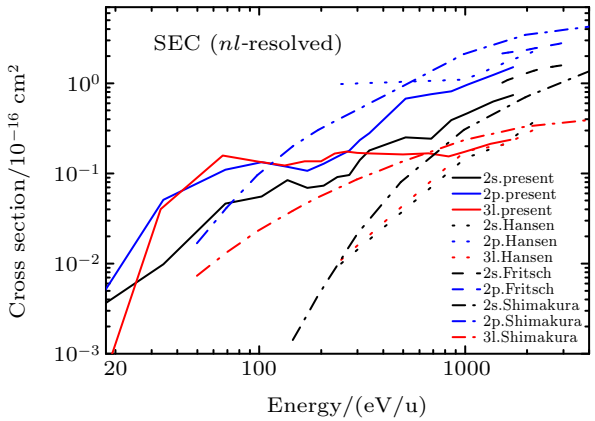

Fig. 10. Comparison between the present state-selective SEC cross sections for the $B^{4+}(1s)$ + $He(1s^2)$ collision with other theoretical[7,8,10] results. Present QMOCC calculation considering the ETF effects (solid line); AOCC results of Hansen *et al.*[7] (dotted line); semi-classical results of Fritsch *et al.*[8] (dashed line) and Shimakura *et al.*[10] (dash dotted line).

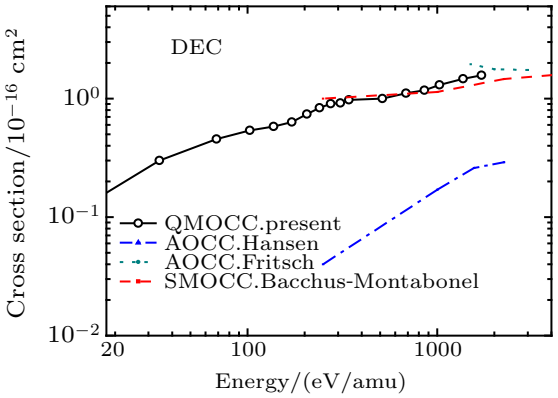

Fig. 11. Comparison between the present DEC cross sections for the $B^{4+}(1s)$ + $He(1s^2)$ collision with other theoretical results.[7–9] Present QMOCC calculation considering the ETF effects (solid line with open circles); AOCC results of Hansen *et al.*[7] (dash dotted line); semi-classical results of Fritsch *et al.*[8] (dotted line); and full electron molecular expansion method of Bacchus-Montabonel[9] (dashed line).

For the $B^{4+}(1s)$ + $He(1s^2)$ system, the DEC processes are also important, the present total DEC cross sections are compared with other theoretical results[7–9] in Fig. 11. It can be observed that the theoretical results of Hansen *et al.*[7] and Fritsch *et al.*,[8] in which semiclassical close-coupling formalism with only two-electron atomic orbitals was used, are much lower and higher than our results, respectively. However, Our results are in good agreement with that of Bacchus-Montabonel[9] in the overlapping energy region, and seem to

be well adapted to describe this system because of the molecular treatment. In our calculations, the full three-electron interactions have been taken into account, and the correlation effects between 1s and 2l orbitals have being included in the configuration-interaction calculation in both calculations of Bacchus-Montabonel[9] and ours.

Figure 12 shows the comparison between the present state-selective DEC cross sections for the $B^{4+}(1s) + He(1s^2)$ collision with other theoretical results.[7–9] Among these DEC processes in the considered energy region, the $B^{2+}(1s2p^2)+ He^{2+}$ state is only weakly populated, since its population occurs at small-impact parameters, and the present calculations of DEC to the $B^{2+}(1s2p^2)+ He^{2+}$ state is shown to be in better agreement with the absolute values obtained by Fritsch *et al.*[8] The cross sections to the $B^{2+}(1s2s^2)+ He^{2+}$ states in the considered energy region show a broad trough around $E = 70$ eV/u. While to the $B^{2+}(1s2s2p)$, the cross sections continue to rise as the energy increases. For $E < 40$ eV/u, the electron capture to the $B^{2+}(1s2s^2) + He^{2+}$ state is dominant, and with the energy increasing, the capture to $B^{2+}(1s2s2p)$ also becomes significant, their values of the cross sections intersect at $E \sim 40$ eV/u and 400 eV/u. Our results for electron capture to $B^{2+}(1s2s^2) + He^{2+}$ and $B^{2+}(1s2s2p) + He^{2+}$ states are in better agreement with the results of Bacchus-Montabonel,[9] since the other calculations[7,8] apparently do not have adequate descriptions of the electron interaction as mentioned.

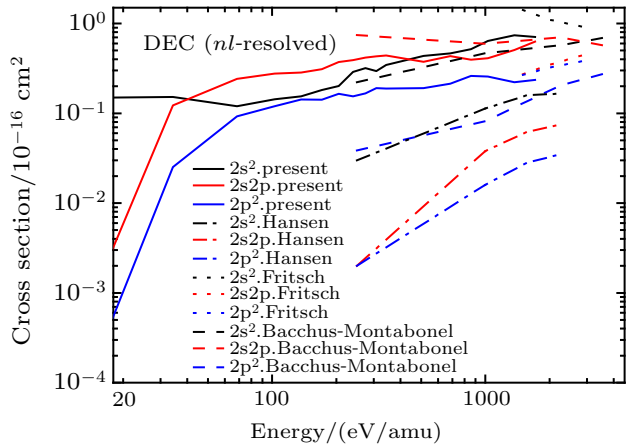

Fig. 12. Comparison between the present state-selective DEC cross sections for the $B^{4+}(1s) + He(1s^2)$ collision with other theoretical results.[7–9] Present QMOCC calculation considering the ETF effects (solid line); AOCC results of Hansen *et al.*[7] (dash dotted line); semiclassical results of Fritsch *et al.*[8] (dotted line); and full electron molecular expansion method of Bacchus-Montabonel[9] (dashed line).

4.3. Comparison between $BeHe^{3+}$ and BHe^{4+} systems

As we have expected, for both of $BeHe^{3+}$ and BHe^{4+} systems, the incident ions have the same number of electrons and collide with the same target, but these two systems have many differences in the collision dynamics because the molecular structures of them are different. We begin the discussion by comparing the total SEC and DEC cross sections. As shown in Fig. 6, for the $Be^{3+}(1s) + He(1s^2)$ collision system, it is observed that only the SEC cross sections are important because the DEC states have large energy gaps with the initial state $Be^{3+}(1s\ ^2S) + He(1s^2)$. The total SEC cross sections have a broad maximum around $E = 150$ eV/u owing to the obvious avoided crossing between the $2\ ^2\Sigma$ and the $1\ ^2\Sigma$ states and the strong radial couplings at $R \sim 5.4$ a.u. (see Figs. 1 and 2). On the other hand, for $B^{4+}(1s) + He(1s^2)$ as shown in Figs. 9 and 11, both of the SEC and DEC processes are important because of the small energy gap with the initial state $B^{4+}(1s\ ^2S) + He(1s^2)$ (see Table 2). In our considered energy region, with the energy decreasing, the SEC and DEC cross sections decrease rapidly, which is consistent with the previous discussion that there is no strong coupling at large internuclear distances.

In order to study the differences between the two systems further, the state-selective cross sections are compared. For the SEC process of the $Be^{3+}(1s) + He(1s^2)$ collision system, electron capture to the $Be^{2+}(1s2s)$ state is dominant and the cross sections have a broad maximum because of the strong radial coupling between $1\ ^2\Sigma$ and $2\ ^2\Sigma$ states. But for BHe^{4+} system, in the considered energy region, with the energy increasing, the cross sections to 2s and 2p states are also increasing, since there are no effective avoided crossings for $R > 4.0$ a.u. and when the internuclear distance $R < 4.0$ a.u., the potentials for 1–4 $^2\Sigma$ and the initial state become very close, the radial couplings between them play a role in the high collision energy region. Moreover, the cross sections to the $Be^{2+}(1s3l) + He^{+}(1s)$ states are not considered as their energies lie relatively high above the initial state $Be^{3+}(1s\ ^2S) + He(1s^2)$. But for $B^{4+}(1s) + He(1s^2)$, although the $B^{3+}(1s3l) + He^{+}(1s)$ states energetically lie very close to the initial state $B^{4+}(1s\ ^2S) + He(1s^2)$ at large internuclear distances, the cross sections for capture to 3l states are relatively small because there is no strong radial coupling between the 3l states with the initial state at the considered distances.

5. Conclusion

This paper studied and compared the nonradiative electron capture processes of the $Be^{3+}(1s)$/ $B^{4+}(1s) + He(1s^2)$ collision systems by using the QMOCC method. Total and state-selective cross sections have been calculated in the energy range 10–1800 eV/u. And the MRD-CI method was used to compute the *ab initio* potential curves and nonadiabatic coupling matrix elements, the largest error in the relative asymptotic energies of these system is about 0.179 eV, which would be sufficient for the scattering calculations. The differences between these two systems in the molecular structure calculations and the dynamic calculation were analyzed. For

$Be^{3+}(1s) + He(1s^2)$, only SEC states are important and the total cross sections have a broad maximum around $E = 150$ eV/u because of the strong radial coupling between $1\ ^2\Sigma$ and $2\ ^2\Sigma$ states at $R \sim 5.4$ a.u. For $B^{4+}(1s) + He(1s^2)$, the SEC and DEC processes are important, and in our considered energy region, with the energy decreasing, the cross sections also decrease rapidly due to no strong coupling at large internuclear distances.

The results agree well with the available experimental data (for $B^{4+}(1s) + He(1s^2)$[11]). For the collision system $Be^{3+}(1s) + He(1s^2)$, our results are in general agreement with those of Suzuki *et al.*[5] in the overlapping energy range. On the other hand, for $B^{4+}(1s) + He(1s^2)$, the QMOCC results are in good agreement with those of Bacchus-Montabonel[9] and seem to be well adapted to describe this system because all the three-electron interactions have been taken into account and the correlation effects between 1s and 2l orbitals have being included in the configuration-interaction calculation, while in the works of Hansen *et al.*[7] and Fritsch *et al.*,[8] semiclassical close-coupling formalism with only two-electron atomic orbitals was used.

References

[1] Winter H 1975 *Vacuum* **25** 497
[2] Keilhacker M, *et al.* 2001 *Nucl. Fusion* **41** 1925
[3] Shimada M, *et al.* 2007 *Nucl. Fusion* **47** S1
[4] Kupriyanov I B, Nikolaev G N, Kurbatova L A, Porezanov N P, Podkovyrov V L, Muzichenko A D, Zhitlukhin A M, Gervash A A and Safronov V M 2015 *J. Nucl. Mater.* **463** 781
[5] Suzuki S, Shirai T and Kimura M 1998 *J. Phys. B: At. Mol. Opt. Phys.* **31** 1741
[6] Shimakura N, *et al.* 1996 *Phys. Scr.* **T62** 39
[7] Hansen J P and Taulbjerg K 1993 *Phys. Rev. A* **47** 2987
[8] Fritsch W and Lin C D 1992 *Phys. Rev. A* **45** 6411
[9] Bacchus-Montabonel M C 1996 *Phys. Rev. A* **53** 3667
[10] Shimakura N, *et al.* 2001 *Phys. Scr.* **T92** 410
[11] Iwai T, Kaneko Y, Kimura M, Kobayashi N, Ohtani S, Okuno K, Takagi S, Tawara H and Tsurubuchi S 1982 *Phys. Rev. A* **26** 105
[12] Krebs S and Buenker R J 1995 *J. Chem. Phys.* **103** 5613
[13] Buenker R J and Phillips R A 1985 *J. Mol. Struct.: THEOCHEM* **123** 291
[14] Dunning T H 1989 *J. Chem. Phys.* **90** 1007
[15] Woon D E and Dunning T H 1994 *J. Chem. Phys.* **100** 2975
[16] Buenker R J and Peyerimhoff S D 1974 *Theor. Chim. Acta* **35** 33
[17] Kramida A, Ralchenko Yu 2017 *Reader J. NIST ASD Team. NIST At. Spectra Database* (ver. 5.5.1)
[18] Herrero B, Cooper I L and Dickinson A S 1996 *J. Phys. B: At. Mol. Opt. Phys.* **29** 5583
[19] Zygelman B and Dalgarno A 1986 *Phys. Rev. A* **33** 3853
[20] Kimura M and Lane N F 1989 *Adv. At. Mol. Phys.* **26** 79
[21] Heil T G, Butler S E and Dalgarno A 1981 *Phys. Rev. A* **23** 1100
[22] Johnson B R 1973 *J. Comput. Phys.* **13** 445
[23] Errea L F, Mendez L and Riera A 1982 *J. Phys. B: At. Mol. Phys.* **15** 101
[24] Errea L F, Harel C, Jouini H, Mendez L, Pons B and Riera A 1994 *J. Phys. B: At. Mol. Opt. Phys.* **27** 3603
[25] Gargaud M, McCarroll R and Valiron P 1987 *J. Phys. B: At. Mol. Phys.* **20** 1555
[26] Bransden B H, McDowell M R C *Charge exchange, the theory of ion-atom collisions* (Clarendon and Oxford 1992)
[27] Bacchus-Montabonel M C and Ceyzeriat P 1998 *Phys. Rev. A* **58** 1162
[28] Yan L L, Wu Y, Qu Y Z, Wang J G and Buenker R J 2013 *Phys. Rev. A* **88** 022706
[29] Gao J W, Wu Y, Sisourat N, Wang J G and Dubois A 2017 *Phys. Rev. A* **96** 052703